PHYSICAL REVIEW E **70**, 045201(R) (2004)

Entanglement and chaos in a square billiard with a magnetic field

Marcel Novaes and Marcus A. M. de Aguiar
Instituto de Física "Gleb Wataghin," Universidade Estadual de Campinas, 13083-970 Campinas, São Paulo, Brazil
(Received 14 July 2004; published 26 October 2004)

We study the dynamical entanglement between the spin and the spatial degrees of freedom for a spin-1/2 charged particle in a square billiard, subject to a nonhomogeneous magnetic field, a system which is classically nonintegrable. This system has three degrees of freedom, one of them being strictly quantum, and we consider initial states which are coherent states with spin in the x direction. The center of the coherent state can be chosen to lie on classically chaotic or regular initial conditions. We show that for chaotic initial conditions the entanglement is rather fast and increases monotonically, while for the regular ones it may present strong recoherences, whose period is related to the classical motion. We also show that this system exhibits special initial conditions which entangle even faster than a typical chaotic one.

DOI: 10.1103/PhysRevE.70.045201 PACS number(s): 05.45.Mt, 03.65.Ud

Recent technological advances have made it possible to create and manipulate individual quantum states in the laboratory, thus allowing direct observations of entanglement and decoherence [1], concepts that are central to quantum computation and quantum information [2]. Dynamical generation of entanglement and its relation to classical chaos has been the subject of many recent investigations. Furuya *et al.* [3] have studied the Jaynes–Cummings model without the rotating-wave approximation, and found the entanglement rate to be greater for quantum states centered on classically chaotic initial conditions. In later works [4,5] they have shown that a regular initial condition can sometimes lead to faster entanglement than a chaotic one and that recoherences were related to the compactness of the spin degree of freedom.

In the past few years much work has been done in this area [6], and also about the relation between decoherence and fidelity, a measure of a system's sensitivity to perturbations. If a state $|\psi_0\rangle$ evolves under the action of two different Hamiltonians H_1 and H_2, then the overlap

$$|\langle\psi_1|\psi_2\rangle|^2 = |\langle\psi_0|e^{iH_1t_1/\hbar}e^{-iH_2t_2/\hbar}|\psi_0\rangle|^2 \tag{1}$$

depends on t_1 and t_2 and has been suggested as a good measure of quantum chaoticity. One typically considers $t_1=t_2$, in which case this can be considered as a time-reversal experiment and (1) is called the quantum fidelity or the "Loschmidt echo." Jalabert and Pastawski showed [7] that its decay depends on the classical Lyapunov exponent for a narrow wave packet in a chaotic region of phase space. Since then, many different decay regimes have been investigated [8]. The connection with decoherence comes as follows: if $|\psi_0\rangle$ is seen as the initial state of some "environment," then its ability to induce decoherence upon some system is given by the overlap (1), as analyzed for example in [9,10].

Most of these previous works have considered the interaction of two subsystems, D_1 and D_2, or systems with two degrees of freedom. The system we study here is a spin-1/2 charged particle in a square billiard. This system has three degrees of freedom: two spatial ones, which have a very well-defined classical limit, and the spin, which is strictly quantum. We consider the entanglement between the spin degree of freedom D_2 and the spatial degrees of freedom D_1, in the case when only D_1 can have chaotic dynamics. Coupling of a qubit or a pair of qubits to a chaotic environment has been studied for example in [11,12].

On the other hand, in studies of quantum fidelity decay the classical dynamics of H_1 and H_2 in Eq. (1) are always assumed to be qualitatively the same, i.e., initial conditions (IC) that behave regularly for H_1 also behave regularly for H_2 and the same holds for the chaotic ones. This is intuitive if H_2 is seen as a slightly perturbed version of H_1. In the present case, however, this is not always true. We shall construct Hamiltonians, corresponding to spin up and spin down, whose phase spaces have regions which are regular and stable for one Hamiltonian but chaotic for the other. For ICs in this region the amount of entanglement grows faster than for a purely chaotic IC.

We consider a spin-1/2 charged particle (with mass $m=1$ and charge $q=1$) confined to a two-dimensional (2D) square-shaped quantum well of side L, subject to a nonhomogeneous perpendicular magnetic field, so that the Hamiltonian inside the well is (we use units in which $\hbar=1$)

$$H = \frac{1}{2}[\vec{p} - \vec{A}(x,y)]^2 + \epsilon\vec{B}(x,y)\cdot\vec{S}, \tag{2}$$

where

$$\vec{A}(x,y) = (\lambda y^3/3 - B_0 y/2)\hat{x} + (-\lambda x^3/3 + B_0 x/2)\hat{y} \tag{3}$$

is the vector potential corresponding to the magnetic field

$$\vec{B}(x,y) = (B_0 - \lambda x^2 - \lambda y^2)\hat{z}, \tag{4}$$

and the coordinates x and y are measured in units of L.

The parabolic profile of the magnetic field is given by λ, which is also responsible for the coupling between the spin and the orbital motion. The magnitude of B_0 controls the amount of chaos. Since $\vec{B}$ is in the $\hat{z}$ direction the S_z component of the spin is conserved, and the Hamiltonian is block diagonal in the $\{|+\rangle,|-\rangle\}$ basis (denoting "spin up" and "spin down," respectively). It is natural to define

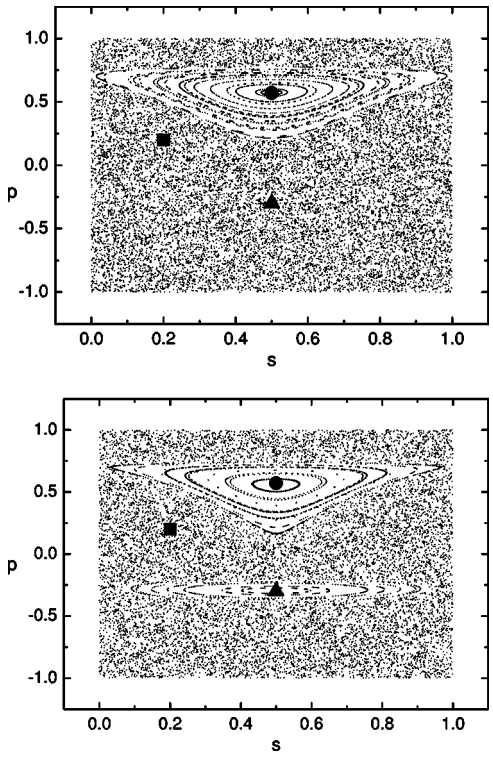

FIG. 1. Poincaré sections for $B_0=77$ and $\lambda=25$ ("spin up" on top). The arc length s is measured in units of the side L. We use the points denoted by ● (regular), ■ (chaotic), and ▲ ("mixed") as initial conditions for the quantum wave packet.

$$H_{\pm}=\frac{1}{2}[\vec{p}-\vec{A}(x,y)]^2\pm\frac{\epsilon}{2}(B_0-\lambda x^2-\lambda y^2), \tag{5}$$

because any initially separable state like $|\psi\rangle(|+\rangle+|-\rangle)$ will evolve according to

$$e^{-iHt}|\psi\rangle(|+\rangle+|-\rangle)=e^{-iH_+t}|\psi\rangle|+\rangle+e^{-iH_-t}|\psi\rangle|-\rangle, \tag{6}$$

and therefore will become entangled with time. Note that H_+ and H_- play the role of the previous H_1 and H_2.

In what follows we will consider $|\psi\rangle$ to be a coherent state $|z_x,z_y\rangle$. Coherent states are minimum-uncertainty states that provide a natural phase-space description of quantum mechanics [13]. They correspond to Gaussian wave functions

$$\langle x,y|z_x,z_y\rangle=\frac{1}{b\sqrt{\pi}}\exp\{-|\vec{r}-\vec{r}_0|^2/2b^2+i\vec{r}_0\cdot\vec{p}\}, \tag{7}$$

where $\vec{r}=(x,y)$, $\vec{r}_0=(x_0,y_0)$, $\vec{p}=(p_x,p_y)$, and

$$z_x=\frac{x_0}{b\sqrt{2}}+i\frac{bp_x}{\sqrt{2}},\quad z_y=\frac{y_0}{b\sqrt{2}}+i\frac{bp_y}{\sqrt{2}}. \tag{8}$$

Note that we use equal variances $b_x=b_y=b$ in both directions.

In the semiclassical limit, and for short times, the evolution (6) will, according to Ehrenfest's theorem, depend on the classical dynamics of H_+ and H_-. In Fig. 1 we show Poincaré sections, or bouncing maps, for both these Hamiltonians, where we have used $B_0=77$, $\lambda=25$, $\epsilon=50$, and all ICs have the same energy $E=10^4$. These values are chosen so that the dynamics is in the semiclassical regime, in the sense that the wave packet can collide with the walls a few times before spreading significantly (we shall comment more on these choices later). In Fig. 1 the x axis shows the arc length s (in units of the side) along the boundary where the collision occurs, counted from the lower left corner of the square, and the y axis shows the cosine of the angle between the tangent of the trajectory just after the collision and the corresponding side of the square [14]. In the following we will use the ICs marked with ● (regular), ■ (chaotic), and ▲ (regular in H_- but chaotic in H_+, which we call "mixed") for the center of our initial coherent state, and we set the dispersion $b=0.1$. Let us denote by τ the period of the ● orbit at this energy and measure time in units of τ.

In order to quantify entanglement we use the linear entropy δ, defined in terms of a partial trace [3,15],

$$\delta=1-\mathrm{Tr}_2\rho_2^2, \tag{9}$$

where ρ_2 is the reduced density matrix of subsystem D_2, given by $\rho_2=\mathrm{Tr}_1\rho$. How fast δ grows indicates how fast subsystem D_2 suffers decoherence due to the entanglement with subsystem D_1. Notice that we take D_1 as the spatial degrees of freedom; we are thus tracing out the chaotic subsystem. If we take the spin component at $t=0$ to be $(|+\rangle+|-\rangle)/\sqrt{2}$ and define

$$e^{-iH_{\pm}t}|z_x,z_y\rangle=|\vec{z}_{\pm}(t)\rangle, \tag{10}$$

then the linear entropy at time t is given by

$$\delta(t)=\frac{1-|\langle\vec{z}_+(t)|\vec{z}_-(t)\rangle|^2}{2}. \tag{11}$$

We see that the entanglement process is governed by the overlap between the coherent state propagated with H_+ and the same state propagated with H_-, the quantum fidelity. Usually, when studying fidelity one considers a change in the Hamiltonian caused by a variation in some external parameter. In the present study this is not the case, since the existence of two different Hamiltonians is due to the intrinsic spin of the particle. Therefore, the relation between fidelity and entanglement appears naturally here. We also note that in the present case the difference between H_+ and H_- is controlled by λ and need not be small in principle.

We now place our coherent state in the chaotic IC denoted by ■ in Fig. 1. Initially we have $|\vec{z}_+(0)\rangle=|\vec{z}_-(0)\rangle$ and $\delta=0$, indicating no entanglement. As time passes, $|\vec{z}_+(t)\rangle$ and $|\vec{z}_-(t)\rangle$ evolve differently, both becoming distorted and less localized, leading to an increase in δ. After some time the initial states have spread all over the square, and δ saturates to a maximum value of 0.5, which corresponds to orthogonality between $|\vec{z}_+(t)\rangle$ and $|\vec{z}_-(t)\rangle$.

In Fig. 2(a) we see the probability density $|\langle x,y|\vec{z}_+(t)\rangle|^2$ at $t=25\tau$. It is randomly distributed through the square. The corresponding density for $|\vec{z}_-(t)\rangle$ is very similar, although orthogonal to this one. In Fig. 3 we see the corresponding evolution of δ (dashed line), which saturates very fast.

If we place the coherent state on the IC denoted by ● in Fig. 1, the situation is different. A classical probability dis-

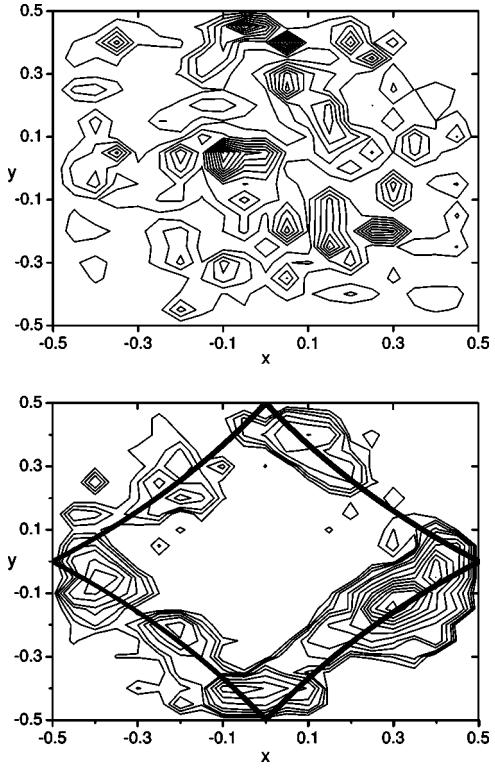

FIG. 2. Probability density $|\langle x,y|\vec{z}_+(t)\rangle|^2$ for the chaotic initial condition (top) and for the regular one (bottom) at $t=25\tau$. The parameters are the same as in Fig. 1. The solid line is the periodic classical trajectory.

tribution centered close to the periodic orbit would be bound to stay inside the regular island: it could not leak into the chaotic sea. A quantum wave function may tunnel to classically forbidden regions, but this takes place on a very large time scale. Therefore, instead of spreading all over the square, it remains localized around the classical trajectory for some time. We can verify this by looking at the probability density $|\langle x,y|\vec{z}_+(t)\rangle|^2$, shown in Fig. 2(b) for $t=25\tau$. The state $|\vec{z}_-(t)\rangle$ is also localized.

The effect of this localization upon entanglement is clear. We see in Fig. 3 the evolution of δ as a solid line. The first important difference between the chaotic and regular cases is

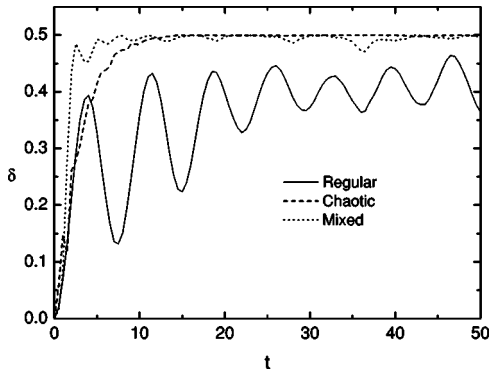

FIG. 3. Linear entropy as a function of time (in units of the basic period τ), for the regular (solid line), chaotic (dashed line), and mixed (dotted line) initial conditions, depicted in Fig. 1.

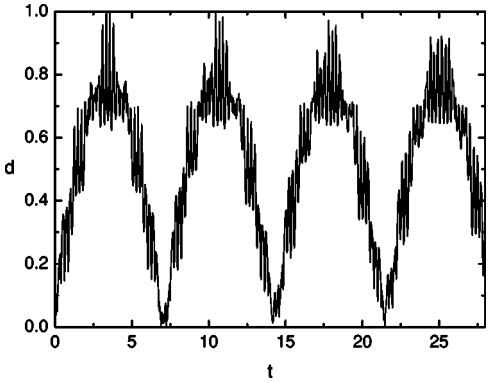

FIG. 4. Distance $d(t)=|\vec{r}_+(t)-\vec{r}_-(t)|$ between the two regular ICs. Besides the period of the orbit there is another time scale, which corresponds to the quantum recoherences.

that the latter takes a much longer time to saturate compared to the first. Another important difference is the presence of recoherences. Furuya *et al.* [5] have studied recoherences in the Jaynes–Cummings model, and concluded that the time scale was related to the compactness of the spin phase space. Even though we are also dealing with a spin, the reason for the recoherences here is completely different. Let us assume that $|\vec{z}_\pm(t)\rangle$ approximately follows a classical trajectory in configuration space given by $\vec{r}_\pm(t)=[x_\pm(t),y_\pm(t)]$, and let us calculate the distance

$$d(t)=|\vec{r}_+(t)-\vec{r}_-(t)| \tag{12}$$

between these classical particles as a function of time. Since they have different energies, they rotate with different periods, as we can see from Fig. 4. The particles start at the same point, and they are again at the same point at $t\simeq 7\tau$. The recoherence time is equal to this time.

Finally, we place our initial coherent state in the special IC marked with a ▲. It is periodic and stable in the H_- dynamics but chaotic in the H_+ dynamics. Therefore $|\vec{z}_-(t)\rangle$ remains trapped inside the regularity island, but $|\vec{z}_+(t)\rangle$ is free to spread over the chaotic sea. This produces a fast entanglement, even faster than that associated with the purely chaotic

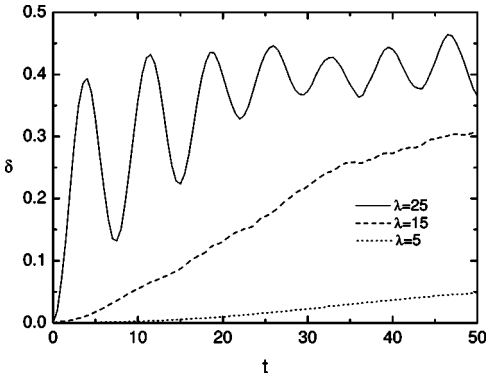

FIG. 5. Linear entropy as a function of time (in units of the basic period τ) for the regular initial condition and different values of λ.

IC, as we can see in Fig. 3. It has only small, erratic oscillations.

We have also considered smaller values of the nonhomogeneity parameter λ, and we can see its influence on the entanglement rate of the regular initial condition in Fig. 5. For small values of λ the dynamics of H_- and H_+ are very similar, and thus the amount of entanglement grows slowly. Also the energy difference between $|\vec{z}_-(t)\rangle$ and $|\vec{z}_+(t)\rangle$ is smaller, and therefore the recoherence time may become much larger than the Ehrenfest time, so that all recoherences vanish and $\delta(t)$ grows almost monotonically. We do not show chaotic ICs because the analysis would be essentially the same. We also do not consider any mixed IC because the stability island involved becomes too small as λ decreases.

In summary, we have studied the dynamical generation of entanglement for a system with three degrees of freedom, one of them being strictly quantum and the others being classical and displaying chaotic behavior. We have calculated the entanglement by tracing out the space, and this leads to a very natural connection between deterministic entanglement and quantum fidelity for this system. Chaotic initial conditions were seen to entangle in a fast and monotonic way, while regular ones may present strong recoherences, whose time scale is related to the classical motion. We have also shown special initial conditions which entangle faster than a typical chaotic one.

Finally, we note that billiards of this type should be accessible to experiment, using semiconductor quantum dots [16]. For a square well on $GaAs/Al_xGa_{1-x}As$ of 1 μm in length the parameters we used correspond to energies of the order of 10 meV and magnetic fields B_0 of the order of 20 mT. The coupling constant ϵ is fixed by the magnetic moment of the electron, but the parabolic parameter λ can be adjusted to enhance the coupling effect.

We acknowledge financial support from Fapesp (Fundação de Amparo à Pesquisa do Estado de São Paulo) and from CNPq (Conselho Nacional de Desenvolvimento Científico e Tecnológico).

[1] M. Brune *et al.*, Phys. Rev. Lett. **77**, 4887 (1996); J. M. Raimond, M. Brune, and S. Haroche, *ibid.* **79**, 1964 (1997); C. A. Sackett *et al.*, Nature (London) **404**, 256 (2000); J. M. Raimond, M. Brune, and S. Haroche, Rev. Mod. Phys. **73**, 565 (2001); B. Julsgaard, A. Kozhekin, and E. P. Polzik, Nature (London) **413**, 400 (2001); J.-W. Pan *et al.*, *ibid.* **423**, 417 (2003); B. B. Blinov *et al.*, *ibid.* **428**, 153 (2004).

[2] M. A. Nielsen and I. L. Chuang, *Quantum Computation and Quantum Information* (Cambridge University Press, Cambridge, 2000).

[3] K. Furuya, M. C. Nemes, and G. Q. Pellegrino, Phys. Rev. Lett. **80**, 5524 (1998).

[4] R. M. Angelo *et al.*, Phys. Rev. E **60**, 5407 (1999).

[5] R. M. Angelo *et al.*, Phys. Rev. A **64**, 043801 (2001).

[6] P. A. Miller and S. Sarkar, Phys. Rev. E **60**, 1542 (1999); A. Tanaka, H. Fujisaki, and T. Miyadera, *ibid.* **66**, 045201(R) (2002); J. N. Bandyopadhyay and A. Lakshminarayan, Phys. Rev. Lett. **89**, 060402 (2002); H. Fujisaki, T. Miyadera, and A. Tanaka, Phys. Rev. E **67**, 066201 (2003); M. Žnidarič and T. Prosen, J. Phys. A **36**, 2463 (2003); J. N. Bandyopadhyay and A. Lakshminarayan, Phys. Rev. E **69**, 016201 (2004).

[7] R. A. Jalabert and H. M. Pastawski, Phys. Rev. Lett. **86**, 2490 (2001).

[8] P. Jacquod, P. G. Silvestrov, and C. W. J. Beenakker, Phys. Rev. E **64**, 055203 (2001); F. M. Cucchietti *et al.*, *ibid.* **65**, 046209 (2002); F. M. Cucchietti, H. W. Pastawski, and D. Wisniacki, *ibid.* **65**, 045206(R) (2002); D. A. Wisniacki and D. Cohen, *ibid.* **66**, 046209 (2002); J. Emerson *et al.*, Phys. Rev. Lett. **89**, 284102 (2002); R. Sankaranarayanan and A. Lakshminarayan, Phys. Rev. E **68**, 036216 (2003); W. Wang, G. Casati, and B. Li, *ibid.* **69**, 025201(R) (2004); G. Veble and T. Prosen, Phys. Rev. Lett. **92**, 034101 (2004); P. Jacquod, *ibid.* **92**, 150403 (2004).

[9] W. H. Zurek, Nature (London) **412**, 712 (2001).

[10] F. M. Cucchietti *et al.*, Phys. Rev. Lett. **91**, 210403 (2003).

[11] T. Prosen, T. H. Seligman, and M. Žnidarič, Phys. Rev. A **67**, 042112 (2003).

[12] J. Lages, V. V. Dobrovitski, and B. N. Harmon, quant-ph/0406001 (unpublished).

[13] J. R. Klauder and B.-S. Skagerstam, *Coherent States: Applications in Physics and Mathematical Physics* (World Scientific, Singapore, 1985).

[14] M. A. M. de Aguiar, Phys. Rev. E **53**, 4555 (1996).

[15] W. H. Zurek, S. Habib, and J. P. Paz, Phys. Rev. Lett. **70**, 1187 (1993).

[16] R. Crook *et al.*, Phys. Rev. Lett. **91**, 246803 (2003).